Journal of Materials Science and Chemical Engineering, 2024, 12, 84-93
https://www.scirp.org/journal/msce
ISSN Online: 2327-6053
ISSN Print: 2327-6045

Preparation of Corncob-Like WO_3 Nanomaterials and Their Photocatalytic Treatment of Toluene

Jianhai Wang[1], Lu Lu[1], Bing Xu[1*], Hongfeng Xu[1], Hongwen Liu[2]

[1]Liaoning Provincial Key Laboratory of Metal Air New Energy Battery, Dalian Jiaotong University, Dalian, China
[2]Dalian Ecological Environment Monitoring Center of Liaoning Province, Dalian, China
Email: *xb@djtu.edu.cn

How to cite this paper: Wang, J.H., Lu, L., Xu, B., Xu, H.F. and Liu, H.W. (2024) Preparation of Corncob-Like WO_3 Nanomaterials and Their Photocatalytic Treatment of Toluene. *Journal of Materials Science and Chemical Engineering*, **12**, 84-93.
https://doi.org/10.4236/msce.2024.122007

Received: January 27, 2024
Accepted: February 26, 2024
Published: February 29, 2024

Abstract

Corn rod-like WO_3 nanomaterials were successfully synthesized by a simple hydrothermal method. The morphology, structure and optical absorption properties of the prepared samples were characterized by SEM, XRD, FTIR and UV-Vis-DRS. The WO_3 materials were corn rod-like morphology with about 800 nm for length and 150 nm for diameter, especially there were plenty of corn particles (about 20 nm) on the surface of corn rods. The X-ray diffraction peaks of the products corresponded with WO_3 standard card, and the characteristic peak of W-O bond was found in the infrared spectrum. The absorption band edge of the products was about 480 nm, indicating their potential visible-light-induced photocatalytic activity. *In situ* FTIR technology research showed that the prepared WO_3 nanomaterials had visible photocatalytic activity to gas-phase toluene. After a photocatalytic reaction for 8 hours toluene was effectively degraded, and carboxylic acid and aldehyde could be regarded as the intermediate products, and CO_2 was produced as the final product during the reaction process.

Keywords

WO_3 Nanomaterials, Visiblelight, Photocatalytic Degradation, Toluene, *In Situ* FTIR

1. Introduction

WO_3 is an N-type semiconductor functional material, which has a strong absorption effect on the solar spectrum compared with the widely studied wide-band gap TiO_2 ($E_g \approx 3.2$ eV) material. WO_3 also has the advantages of non-toxicity,

stable physical and chemical properties, good photochromism, gas sensitivity and photocorrosion resistance, so it is used as a photocatalyst for solar cells [1], gas sensitive elements [2], visible light decomposition of water [3] and degradation of organic matter [4].

NanoWO_3 with various micro morphology has been successfully prepared. Soultanidis [5] synthesized ultrafine tungsten oxide nanoparticles by solvothermal method, generating small tungsten oxide nanoparticles in the presence of organic oxidant trimethylamine N-oxide, and generating tungsten oxide nanorods in the presence of reducing agent 1, 12-dodecarbon diol. Kim [6] synthesized nano-sea urchin-shaped tungsten oxide containing $W_{18}O_{49}$ and WO_3 and studied their electrochromic properties. Li [7] synthesized WO_3 nanorods by simple microwave-assisted hydrothermal method using Na_2SO_4 as structural guide agent and investigated its excellent ethanol sensing characteristics. WO_3 is an N-type semiconductor, and its optical absorption band edge is in the visible light region (E_g = 2.5~2.8 eV). It has many advantages suitable for visible light catalysis, such as deep valence band position (+3.1 eV), strong absorption ability of solar spectrum, stable physical and chemical properties, strong resistance to photocorrosion, etc. Kim [8] used self-assembled polystyrene (PS) colloidal as organic template and polyethylene glycol (PEG) as surfactant to prepare WO_3 film and studied its excellent photoelectric catalytic ability under ultraviolet visible sunlight irradiation.

Toluene is one of the most common volatile organic compounds (VOCs) found in industrial emissions, indoor air and exhaust from motor vehicles. The adverse health effects of toluene on the human body depend on the conditions of exposure, and serious cases may cause nerve damage and sensory disorders [9]. Heterogeneous photocatalytic methods can treat environmental pollutants under mild conditions, and different catalysts have been used to study the photocatalytic degradation and removal of toluene [10] [11] [12] [13]. *In-situ* Fourier transform infrared spectroscopy (FTIR) technology can monitor the surface adsorbents, transition states and intermediates, further speculate the possible reaction pathways and mechanisms. Among them, transmission infrared spectroscopy is a commonly used method to study photocatalytic and thermocatalytic adsorption and reaction [14] [15] [16], and *in situ* diffuse reflection infrared spectroscopy (DRIFT) and attenuated total reflection infrared spectroscopy (ATR-IR) are two effective methods to detect species on the catalyst surface and in the gas phase [17] [18] [19]. In this paper, maize cob WO_3 nanomaterial was synthesized by simple hydrothermal method, and the photocatalytic degradation of toluene under visible light irradiation was studied by *in situ* infrared spectroscopy.

2. Experimental Part

2.1. Reagents and Instruments

Na_2WO_4, Na_2SO_4, hydrochloric acid (all analytically pure, Sinopharm Chemical

Reagent Co., LTD.), toluene (Analytically pure, Tianjin Kemeiou Chemical Reagent Co., LTD.), and deionized water were used for the experiment.

Quanta 200 FEG Field Emission Environmental Scanning Electron Microscope (ESEM, FEI Company, USA); D/MAX-IIIA X-ray diffractometer (XRD, Shimadzu Company, Japan); VERTEX 70 Fourier Transform infrared spectrometer (BRUKER, Germany); UV550 UV-visible diffuse reflection spectrometer (DRS, JASCO, Japan); DF-101S collector thermostatic heating magnetic stirrer (Gongyi Yuhua Instrument Co., LTD.); TG-WS top high-speed centrifuge (Hunan Xiangyi Experimental Instrument Development Co., LTD.); XQ500W adjustable xenon lamp source (Shanghai Lansheng Electronics Co., LTD.).

2.2. Experimental Process

2.2.1. Preparation of WO_3 Nanomaterials

Add Na_2WO_4 and Na_2SO_4 to 40 mL deionized water, stir them magnetically for 30 min, then drop 3 mol/L hydrochloric acid, and adjust the pH to 2. The mixed solution was poured into the reaction kettle and heated to 190˚C for 24 h. The solution was cooled to room temperature, separated by centrifugation, and washed with deionized water, and dried at 60˚C for 6 h. The light green WO_3 nano powder was obtained by full grinding in an agate mortar.

2.2.2. Characterization of WO_3 Nanomaterials

ESEM was used to characterize the surface morphology of WO_3 nanomaterials. XRD, DRS and FTIR were used to determine the crystallinity, optical absorption characteristics and molecular structure of the prepared samples.

2.2.3. Photocatalytic Performance Test of WO_3 Nanomaterials

The homemade infrared light reaction cell (diameter 4 cm, length 10 cm) consists of two sodium chloride windows and a sample holder (diameter 13 mm). WO_3 nano-powder of 0.05 g was pressed into circular plates and placed on the sample shelf, and 2 μL toluene was injected into the reactor with a microsyringe. After 30 minutes, toluene vapor reaches adsorption equilibrium in the reactor, and Xenon lamp (λ > 400 nm) light source with light intensity of about 50 $mW{\cdot}cm^{-2}$ is turned on. *In situ* FTIR was used to continuously collect infrared spectra with a resolution of 1 cm^{-1} and a scanning range of 4000 - 400 cm^{-1} during the photocatalytic reaction.

3. Results and Discussion

3.1. Morphology and Structure of WO_3 Nanorods

Figure 1 shows the SEM photo of WO_3. According to Figure 1(a), the microstructure of WO_3 is corn-cob shape with good dispersion. It can be observed from Figure 1(b) that the length of nanorods is about 800nm, and the diameter is about 150 nm. The surface of the corn cob is uniformly covered with "corn kernels" with a diameter of about 20 nm.

Figure 2 is the X-ray diffraction pattern of WO_3 nanomaterials, from which

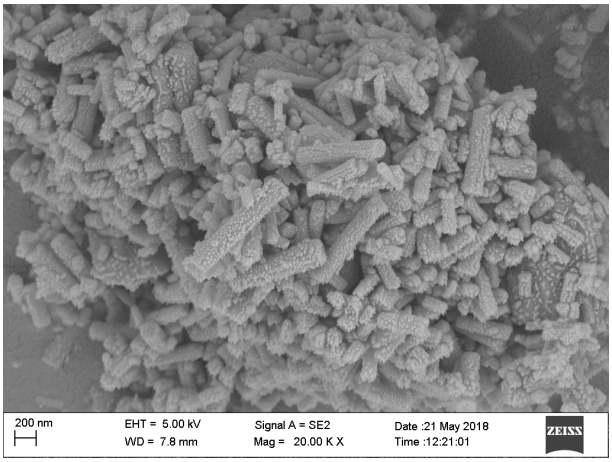

(a)

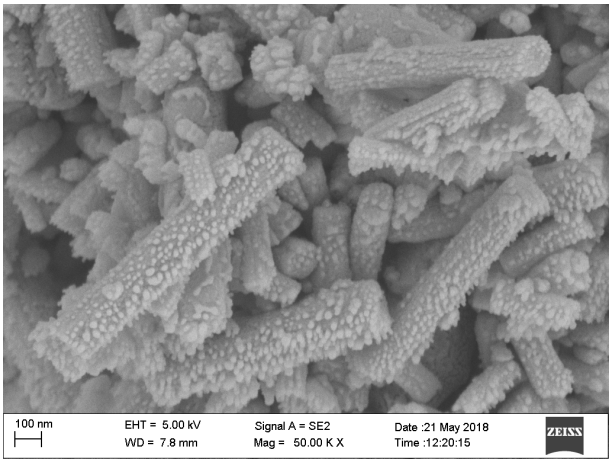

(b)

Figure 1. SEM images of WO_3 nanorods (a) and its local magnification (b).

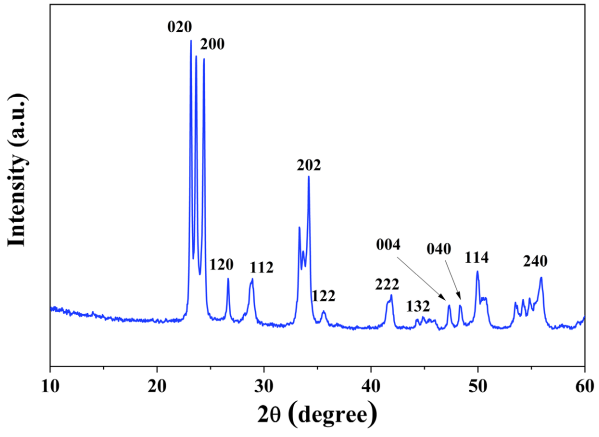

Figure 2. Typical XRD pattern of the prepared WO_3 nanorods.

the crystal planes of (020), (200), (120), (112), (202), (122), (132), (004), (040), (114), (240) can be clearly seen, and each characteristic diffraction peak of the

WO_3 standard card (JCPDS No. 20-1323) corresponded one to one, indicating that WO_3 nanomaterial was successfully synthesized. The shape of each diffraction peak is sharp, which indicates that the crystallinity of the prepared sample is good.

3.2. Infrared and UV-Visible Spectral Characterization of WO_3 Nanorods

Figure 3 shows the infrared representation of WO_3 sample. The absorption peaks at 3443 and 1631 cm^{-1} are attributed to surface hydroxyl and adsorbed water molecules [20], respectively, while the infrared peaks at 2362 cm^{-1} correspond to the adsorbed or trace CO_2 in the atmosphere [21]. It should be particularly pointed out that the peak at 856 cm^{-1} is the characteristic peak of W-O bond [22], indicating that the prepared sample is WO_3 nanomaterial. The upper part of the figure shows the infrared spectrum of the newly prepared WO_3 catalyst, and the lower part shows the infrared spectrum of the catalyst after the photocatalytic reaction for 8 h. It can be seen the position and intensity of each characteristic peak of the two spectral lines almost do not change, indicating that the WO_3 nanocatalyzer is relatively stable.

Figure 4 shows the UV-VIS diffuse absorption spectra of WO_3 sample. It can be seen from the figure that the samples have certain absorption intensity in the UV-visible region. And the absorption band edge is about 480 nm, indicating that the WO_3 sample has potential visible light catalytic activity.

3.3. Visible Light Catalytic Performance of WO_3 Nanorods

Figure 5 shows the infrared spectra of toluene adsorbed on WO_3 catalyst every 5 min from toluene injection into the reactor to 30 min. As shown in the figure, in the full-band mid-infrared spectral region from 4000 to 400 cm^{-1}, toluene has characteristic infrared absorption in the regions of 3250 - 2750 cm^{-1}, 2000 - 1250 cm^{-1}, and 750 - 400 cm^{-1}, and the specific attribution is detailed below. According to the peak heights of each characteristic infrared peak in the figure, toluene

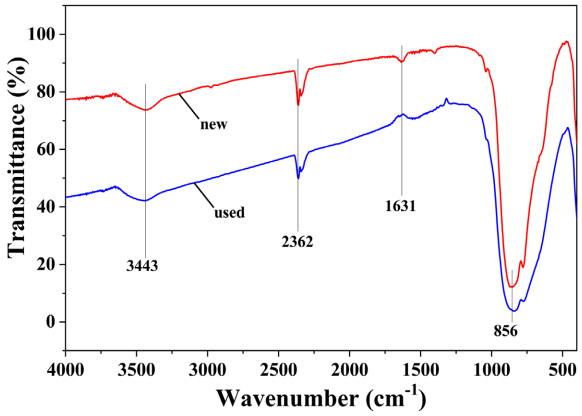

Figure 3. FTIR spectra of the prepared WO_3 nanorods before and after using.

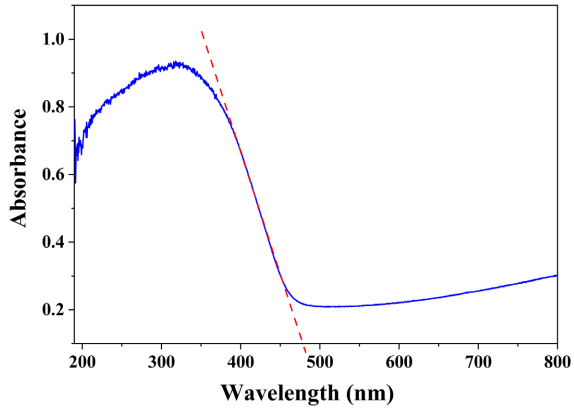

Figure 4. UV-vis diffuse reflection spectrum of the prepared WO_3 nanorods.

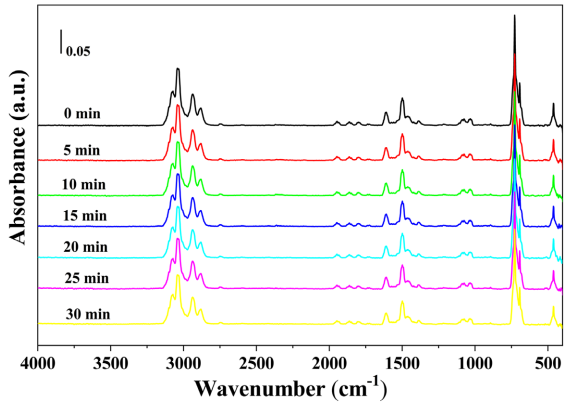

Figure 5. Full-band infrared spectra of toluene adsorption on WO_3 nanorods.

could reach the adsorption-desorption equilibrium on WO_3 catalyst within 30 min.

Figure 6 shows the infrared absorption spectra of toluene in various regions at different times after visible light catalytic degradation on WO_3 nanorods for 8 h with the extension of illumination time. In **Figure 6(a)**, the peaks at 3073, 3043 and 3032 cm^{-1} are attributed to the stretching vibration of C-H bond in benzene ring [23], and the peaks at 2936 and 2880 cm^{-1} are attributed to the stretching vibration peak of C-H bond in toluene methyl group [24]. In **Figure 6(c)**, the peaks at 1948, 1860 and 1801 cm^{-1} are attributed to the out-of-plane deformation vibration peaks of C-H bond on the benzene ring [25], and the peaks at 1610 and 1498 cm^{-1} are attributed to the stretching vibration of the benzene ring skeleton C=C [26]. In **Figure 6(d)**, the infrared peak between 1089 and 1025 cm^{-1} is attributed to the in-plane deformation vibration peak of C-H bond on the benzene ring [27], and the peak at 729 and 695 cm^{-1} is attributed to the characteristic absorption peak of benzene ring mono-substitution [24]. As can be seen from the above three figures, with the increase of the photocatalytic reaction time, the peak heights of each characteristic peak of toluene gradually

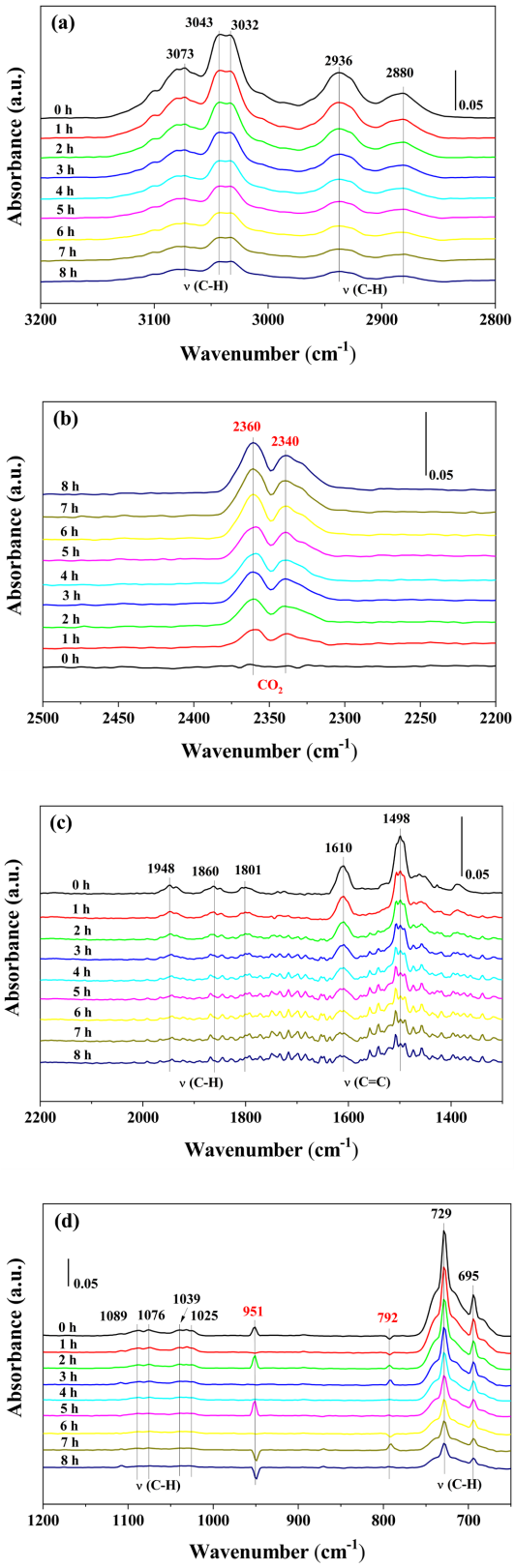

Figure 6. FTIR spectra recorded as a function of irradiation time following the photocatalytic degradation of toluene on WO_3 nanorods in the different regions: (a) 3300 - 2800 cm^{-1}, (b) 2500 - 2200 cm^{-1}, (c) 2200 - 1300 cm^{-1}, (d) 1200 - 650 cm^{-1}.

decreased, indicating that toluene was effectively degraded on WO_3 nanorods catalyst. In addition, it is worth mentioning that as shown in **Figure 6(b)**, the peaks at 2360 and 2340 cm^{-1} are the characteristic peaks of CO_2 [21]. It can be clearly seen that with the prolongation of the reaction time, the peak height of the characteristic peaks of CO_2 increases significantly, indicating that CO_2 is the final product of toluene degradation catalyzed by visible light.

In addition, it should be particularly pointed out that several new infrared peaks appeared in the reaction process. The peak at 951 cm^{-1} was attributed to the out-of-plane deformation vibration of O-H bond in carboxylic acid [28], and the peak at 792 cm^{-1} was attributed to the C-H deformation vibration of aldehyde [29]. According to previous reports [29] and the results of this paper, benzaldehyde and benzoic acid are intermediates of toluene photocatalytic reaction.

4. Conclusions

1) One-step synthesis of corncob WO_3 nanomaterial by hydrothermal method. The rod length is about 800 nm, the diameter is about 150 nm and the surface size of cornlike particles is about 20 nm.

2) The nanomaterials have a certain absorption intensity in the UV-Vis spectral region, and the absorption band edge is around 480 nm, which can effectively use solar energy.

3) *In situ* infrared spectroscopy showed that the adsorption equilibrium of toluene in gas phase was reached on the corncob WO_3 nano-catalyst for 30 min. It could be seen that after 8 h irradiation, each characteristic peak of toluene was significantly weakened, indicating that it was photocatalytically degraded.

4) *In situ* infrared spectrum, the characteristic peaks of reaction intermediates such as carboxylic acid and aldehyde appear simultaneously, and the characteristic peak intensity of the final product CO_2 is significantly increased, indicating that corncob WO_3 nanomaterial can effectively degrade toluene under visible light irradiation.

Conflicts of Interest

The authors declare no conflicts of interest regarding the publication of this paper.

References

[1] Ahn, S.H. and Manthiram, A. (2016) Edge-Oriented Tungsten Disulfide Catalyst Produced from Mesoporous WO_3 for Highly Efficient Dye-Sensitized Solar Cells. *Advanced Energy Materials*, **6**, 1501814-1501820. https://doi.org/10.1002/aenm.201501814

[2] Zen, J., Hu, M., Wang, W.D., *et al*. (2012) NO_2-Sensing Properties of Porous WO_3 Gas Sensor Based on Anodized Sputtered Tungsten Thin Film. *Sensors and Actuators B*: *Chemical*, **161**, 447-452. https://doi.org/10.1016/j.snb.2011.10.059

[3] Solarska, R., Jurczakowski, R., Augustynski, J., *et al*. (2012) Efficient Visible-Light Driven Water Photoelectrolysis System Using a Nanocrystalline WO_3 Photoanode

and a Methane Sulfonic Acid Electrolyte. *Nanoscale*, **4**, 1553-1556. https://doi.org/10.1039/c2nr11573e

[4] Yan, J., Gu, J.M., Wang, X., *et al*. (2017) Design of 3D WO_3/H-BN Nanocomposites for Efficient Visible-Light-Driven Photocatalysis. *RSC Advances*, **7**, 25160-25170. https://doi.org/10.1039/C7RA02929B

[5] Nikolaos, S., Wu, Z., Christopher, J.K., *et al*. (2012) Solvothermal Synthesis of Ultrasmall Tungsten Oxide Nanoparticles. *Langmuir*, **28**, 17771-17777. https://doi.org/10.1021/la3029462

[6] Do-Hyung, K. (2012) Effects of Phase and Morphology on the Electrochromic Performance of Tungsten Oxide Nano-Urchins. *Solar Energy Materials & Solar Cells*, **107**, 81-86. https://doi.org/10.1016/j.solmat.2012.07.030

[7] Li, Y.N., Su, X.T., Jian, J.K., *et al*. (2010) Ethanol Sensing Properties of Tungsten Oxide Nanorods Prepared Bymicrowave Hydrothermal Method. *Ceramics International*, **36**, 1917-1920. https://doi.org/10.1016/j.ceramint.2010.03.016

[8] Jung, K.K., Jun, H.M., Tae-Woo, L., *et al*. (2012) Inverse Opal Tungsten Trioxide Films with Mesoporous Skeletons: Synthesisand Photoelectrochemical Responses. *Chemical Communications*, **48**, 11939-11941. https://doi.org/10.1039/c2cc36984b

[9] Bale, A.S., Meachan, C.A., Benignus, V.A., *et al*. (2005) Volatile Organic Compounds Inhibit Human and Rat Neuronal Nicotinic Acetylcholine Receptors Expressed in Xenopusoocytes. *Toxicology and Applied Pharmacology*, **205**, 77-88. https://doi.org/10.1016/j.taap.2004.09.011

[10] Gao, J., Si, Z.C., Xu, Y.F., *et al*. (2019) Pd-Ag@CeO_2 Catalyst of Core-Shell Structure for Low Temperature Oxidation of Toluene under Visible Light Irradiation. *The Journal of Physical Chemistry C*, **123**, 1761-1769. https://doi.org/10.1021/acs.jpcc.8b09060

[11] María, D.H.A., Isabel, T.T., Juan, M.C., *et al*. (2011) Operando FTIR Study of the Photocatalytic Oxidation of Methylcyclohexane Andtoluene in Air over TiO_2-ZrO_2 Thin Films: Influence of the Aromaticity of the Targetmolecule on Deactivation. *Applied Catalysis B*: *Environmental*, **101**, 283-293. https://doi.org/10.1016/j.apcatb.2010.09.029

[12] Williams, I., Fodjo, E., Narcisse, P., *et al*. (2022) Study of Photocatalytic Activity of a Nanostructured Composite of ZnS and Carbon Dots. *Advances in Nanoparticles*, **11**, 111-128.

[13] Shi, X., Gao, C., Wei, X., *et al*. (2023) Synthesis of CC/$BiPO_4$/Bi_2WO_6 Composite Material and Its Photocatalytic Performance. *Optics and Photonics Journal*, **13**, 156-166. https://doi.org/10.4236/opj.2023.136014

[14] Chen, Y.K., Lin, Y.F., Peng, Z.W., *et al*. (2010) Transmission FT-IR Study on the Adsorption and Reactions of Lactic Acid and Poly(Lacticacid) on TiO_2. *Journal of Physical Chemistry C*, **114**, 17720-17727. https://doi.org/10.1021/jp105581t

[15] Barndõk, H., Merayo, N., Blanco, L., *et al*. (2016) Application of On-Line FTIR Methodology to Study the Mechanisms Ofheterogeneous Advanced Oxidation Processes. *Applied Catalysis B*: *Environmental*, **185**, 344-352. https://doi.org/10.1016/j.apcatb.2015.12.036

[16] Wang, H., Zhang, W.D., Li, X.W., *et al*. (2018) Highly Enhanced Visible Light Photocatalysis and *in Situ* FT-IR Studies on Bi Metal@Defective BiOCl Hierarchical Microspheres. *Applied Catalysis B*: *Environmental*, **225**, 218-227. https://doi.org/10.1016/j.apcatb.2017.11.079

[17] Hägglund, C., Kasemo, B. and Österlund, L. (2005) *In Situ* Reactivity and FTIR Study of the Wet and Dry Photooxidation of Propane on Anatase TiO_2. *Journal of*

Physical Chemistry B, **109**, 10886-10895. https://doi.org/10.1021/jp0442448

[18] Koichumanova, K., Vikla, A.K.K., Cortese, R., *et al*. (2018) *In Situ* ATR-IR Studies in Aqueous Phase Reforming of Hydroxyacetone on Pt/ZrO_2 and Pt/AlO(OH) Catalysts: The Role of Aldol Condensation. *Applied Catalysis B*: *Environmental*, **232**, 454-463. https://doi.org/10.1016/j.apcatb.2018.03.090

[19] Dolamic, I. and Bürgi, T. (2007) Photocatalysis of Dicarboxylic Acids over TiO_2: An *in Situ* ATR-IR Study. *Journal of Catalysis*, **248**, 268-276. https://doi.org/10.1016/j.jcat.2007.03.020

[20] Song, X.F. and Gao, L. (2007) Synthesis, Characterization, and Optical Properties of Well-Defined N-Doped, Hollow Silica/Titania Hybrid Microspheres. *Langmuir*, **23**, 11850-11856. https://doi.org/10.1021/la7019704

[21] Pradeep, A., Priyadharsini, P. and Chandrasekaran, G. (2008) Sol-Gel Route of Synthesis of Nanoparticles of $MgFe_2O_4$ and XRD, FTIR and VSM Study. *Journal of Magnetism and Magnetic Materials*, **320**, 2774-2779. https://doi.org/10.1016/j.jmmm.2008.06.012

[22] Sertkol, M., Köseoğlu, Y., Baykal, A., *et al*. (2010) Synthesis and Magnetic Characterization of $Zn_{0.7}Ni_{0.3}Fe_2O_4$ Nanoparticles via Microwave-Assisted Combustion Route. *Journal of Magnetism and Magnetic Materials*, **322**, 866-871. https://doi.org/10.1016/j.jmmm.2009.11.018

[23] Nagao, M. and Suda, Y. (1989) Adsorption of Benzene, Toluene, and Chlorobenzene on Titanium Dioxide. *Langmuir*, **5**, 42-47. https://doi.org/10.1021/la00085a009

[24] Zhang, H. (2007) Learning Guidance and Comprehensive Practice of Modern Organic Spectrum Analysis. Chemical Industry Process, Beijing, 151-180.

[25] Sivasankar, N. and Vasudevan, S. (2004) Temperature-Programmed Desorption Andinfrared Spectroscopic Studies of Benzene Adsorption in Zeolite ZSM-5. *Journal of Physical Chemistry B*, **108**, 11585-11590. https://doi.org/10.1021/jp048399r

[26] Wu, W.C., Liao, L.F., Lien, C.F., *et al*. (2001) FTIR Study of Adsorption, Thermal Reactionsand Photochemistry of Benzene on Powdered TiO_2. *Physical Chemistry Chemical Physics*, **3**, 4456-4461. https://doi.org/10.1039/b104926g

[27] Gunasekaran, S. and Uthra, D. (2008) Vibrational Spectra and Qualitative Analysis of Albendazole and Mebendazole. *Asian Journal of Chemistry*, **20**, 6310-6324.

[28] Socrates, G. (2004) Infrared and Raman Characteristic Group Frequencies: Tables and Charts. John Wiley and Sons Ltd., London.

[29] Augugliaro, V., Coluccia, S., Loddo, V., *et al*. (1999) Photocatalytic Oxidation of Gaseous Toluene on Anatase TiO_2 Catalyst: Mechanistic Aspects and FT-IR Investigation. *Applied Catalysis B*: *Environmental*, **20**, 15-27. https://doi.org/10.1016/S0926-3373(98)00088-5